

# ScoreMix: Improving Face Recognition via Score Composition in Diffusion Generators

Parsa Rahimi<sup>1,2</sup> Sébastien Marcel<sup>2,3</sup>

## Abstract

In this paper, we propose ScoreMix, a novel yet simple data augmentation strategy leveraging the score compositional properties of diffusion models to enhance discriminator performance, particularly under scenarios with limited labeled data. By convexly mixing the scores from different class-conditioned trajectories during diffusion sampling, we generate challenging synthetic samples that significantly improve discriminative capabilities in all studied benchmarks. We systematically investigate class-selection strategies for mixing and discover that greater performance gains arise when combining classes distant in the discriminator’s embedding space, rather than close in the generator’s condition space. Moreover, we empirically show that, under standard metrics, the correlation between the generator’s learned condition space and the discriminator’s embedding space is minimal. Our approach achieves notable performance improvements without extensive parameter searches, demonstrating practical advantages for training discriminative models while effectively mitigating problems regarding collections of large datasets. Paper website: <https://parsa-ra.github.io/scoremix>.

## 1. Introduction

In recent years, visual generative models have emerged as a cornerstone of modern machine learning, reshaping how machines perceive, synthesize, and manipulate visual data. From photorealistic image generation to high-fidelity video synthesis and 3D reconstruction, these models have demonstrated an unprecedented ability to learn complex visual distributions and produce outputs with remarkable coherence and diversity. Fueled by advancements in deep neural ar-

<sup>1</sup>EPFL, Switzerland <sup>2</sup>Idiap, Switzerland <sup>3</sup>UNIL, Switzerland. Correspondence to: Parsa Rahimi <[parsa.rahiminoshanagh@epfl.ch](mailto:parsa.rahiminoshanagh@epfl.ch)>.

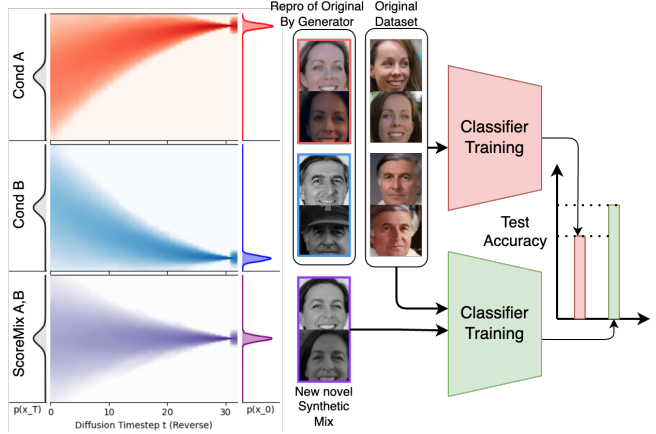


Figure 1. ScoreMixing. The first two subplots on the left show diffusion trajectories obtained under two different conditioning signals (Cond A) and (Cond B). By convexly mixing their score functions (ScoreMix A,B), we generate synthetic samples that interpolate between the two trajectories. Without relying on other sources of information, adding these synthetic augmentations to the original training set boosts the discriminator’s performance.

chitectures—particularly Generative Adversarial Networks (GANs), Variational Autoencoders (VAEs), and, more recently, diffusion-based models—this paradigm has not only achieved impressive technical milestones but has also catalyzed breakthroughs across a wide array of domains. These advancements have further enabled complementary effects from decomposing generative systems into specialized components (e.g., Discrete Diffusion Transformers (Peebles & Xie, 2023), which leverage VQGAN (Esser et al., 2021) for tokenization). Applications now span creative arts, medical imaging, virtual reality, robotics, scientific visualization, and drug discovery, to name a few, highlighting the transformative potential of these models in both research and industry (Lee et al., 2025). The rapid evolution of visual generative models is characterized by a convergence of algorithmic innovation, increased computational resources, and the availability of large-scale datasets. As the field continues to mature, a central challenge lies in understanding and improving the generalization, controllability, and interpretability of these models, particularly when deployed in real-world scenarios.

In many cases, large foundation models cannot be employed due to legal, ethical, or other concerns. In this paper, we focus on scenarios involving limited data, demonstrating how we can increase discriminative power by generating synthetic samples while only using a **single labeled dataset**.

Recently, authors in (Rahimi et al., 2025) proposed AugGen, a method that mixes labels in the condition space of the generator to produce challenging samples for the discriminator. We base our experiments on this approach. A key benefit of AugGen is that final samples can be generated in multiple passes of the diffusion denoiser (e.g., 50 steps) using the same condition mix. However, a downside of this approach, which we highlight in our work, is that the condition space is unstructured, exhibiting little correlation with the learned embedding space of the discriminator. This issue prompted the authors to propose a computationally expensive grid search to find appropriate mixing parameters for different source classes.

In this work, we explore the *score composition phenomenon* in diffusion models (Liu et al., 2022; Bradley et al., 2025) and leverage this property to generate useful synthetic data applied to the task of face recognition (FR). Specifically, our goal is to improve the performance of a discriminative model trained on a labeled dataset augmented with synthetic data generated by a diffusion model trained on the same original real data. Our motivation is to enhance discriminative performance strictly with the *available data*, sidestepping paradigms that rely on pretrained generators such as Stable Diffusion (Esser et al., 2024) or FLUX (Labs, 2024), which typically depend on large datasets. These pretrained models have inherent restrictions and domain-specific limitations (e.g., poor generalization to data outside their training distribution, such as CT images, requiring fine-tuning or other adaptation methods, again implicating generator retraining).

We investigate the following questions:

1. *Can we leverage the score composition phenomenon of generative models to produce challenging samples beneficial for discriminator training?*
2. *When mixing classes, which combinations yield the greatest improvement in discriminator performance?*
3. *Is there a correlation between the learned condition space of a generator and the discriminator’s feature space?*

To the best of our knowledge, these questions have not previously been addressed. Additionally, we believe this is the first study leveraging score composition for data augmentation, demonstrating a significant performance boost in training discriminative models while preventing information leakage.

## 2. Related Work

Early approaches for introducing augmentations, based on generators (per-class GANs (Frid-Adar et al., 2018)), do not scale to thousands of classes. More recent methods include diffusion-model fine-tuning on ImageNet (Azizi et al., 2023), instance-level redraws via text-to-image models (Kupyn & Rupprecht, 2024), and fully labeled 3DMM-based face rendering (Wood et al., 2021; Blanz & Vetter, 1999). Face-recognition-specific pipelines synthesize identities with controllable GAN mixups (SynFace (Qiu et al., 2021)), modeling the latent space of pre-trained StyleGANs (Rahimi et al., 2023), dual-condition diffusion and demographic filtering (DCFace (Kim et al., 2023)), bias-mitigation via StyleGAN2-ADA pretraining (Sevastopolskiy et al., 2023), attribute-conditioned diffusion (ID<sup>3</sup> (Xu et al., 2024)), and 3D-rendered datasets enhanced by image-to-image translation (DigiFace1M and RealDigiFace (Bae et al., 2023; Rahimi et al., 2024)) or CLIP-guided sampling (VariFace (Yeung et al., 2024)).

**Discussion.** Most synthetic FR pipelines rely on external data sources or multi-stage filtering. By contrast, AugGen (Rahimi et al., 2025) demonstrates that performance gains can be achieved using only the original dataset. We build on this insight, introducing ScoreMixing to further enhance discrimination without external data dependencies.

## 3. Method

Following (Rahimi et al., 2025), here we first formally define the notion of a discriminator and a generator trained using the same dataset.

**Discriminator.** Assume a dataset  $\mathbf{D}_{\text{orig}} = \{(\mathbf{X}_i, y_i)\}_{i=0}^{k-1}$ , where each  $\mathbf{X}_i \in \mathbb{R}^{H \times W \times 3}$  and  $y_i \in \{0, \dots, l-1\}$  ( $l < k$ ). The goal is to learn a discriminative model  $f_{\theta_{\text{dis}}} : \mathbf{X} \rightarrow y$  that estimates  $p(y|\mathbf{X})$  (e.g., on ImageNet (Russakovsky et al., 2015) or CASIA-WebFace (Yi et al., 2014)). Typically, similar images have closer features under a distance  $\text{dist}_{\text{emb}}$  (e.g., cosine distance). We train  $f_{\theta_{\text{dis}}}$  via empirical risk minimization:

$$\theta_{\text{dis}}^* = \arg \min_{\theta_{\text{dis}} \in \Theta_{\text{dis}}} \mathbb{E}_{(\mathbf{x}, y) \sim \mathbf{D}_{\text{orig}}} [\mathcal{L}_{\text{dis}}(f_{\theta_{\text{dis}}}(\mathbf{X}), y)], \quad (1)$$

where  $\mathcal{L}_{\text{dis}}$  is typically cross-entropy, and  $\mathbf{h}_{\text{dis}}$  denotes hyperparameters (e.g., learning rates).

**Generative Model.** Generative models seek to learn the data distribution, enabling the generation of new samples. We use diffusion models (Song et al., 2020; Anderson, 1982), which progressively add noise to data and train a Denoiser  $S$ . Following (Karras et al., 2022; 2024b),  $S$  is learned in two stages. First, for a given noise level  $\sigma$ , we add noise  $\mathbf{N}$  to  $E_{\text{pre}}(\mathbf{X})$  (or  $\mathbf{X}$  directly in pixel-based diffusion)

and remove it via:

$$\mathcal{L}(S_{\theta_{den}}; \sigma) = \mathbb{E}_{(\mathbf{X}, y) \sim \mathcal{D}^{\text{orig}}, \mathbf{N} \sim \mathcal{N}(\mathbf{0}, \sigma \mathbf{I})} [\|S_{\theta_{den}}(E_{\text{pre}}(\mathbf{X}) + \mathbf{N}; c(y), \sigma) - \mathbf{X}\|_2^2], \quad (2)$$

where  $c(y)$  denotes the class condition, and  $E_{\text{pre}}(\cdot)$  and  $D_{\text{pre}}(\cdot)$  pre-processing and post-processing functions in terms of Encoder and Decoder (e.g., they can be magnitude normalization or VAE-based compression). In the second stage, we sample different noise levels and minimize:

$$\theta_{den}^* = \arg \min_{\theta_{den} \in \Theta_{den}} \mathbb{E}_{\sigma \sim \mathcal{N}(\mu, \sigma^2)} [\lambda_{\sigma} \mathcal{L}(S_{\theta_{den}}; \sigma)], \quad (3)$$

where  $\lambda_{\sigma}$  weights each noise scale. Here  $c$  amongst the time embedding is learned. For simplicity, we omit the *den* and *dis* subscripts used to distinguish the parameters of the Denoiser and Discriminator, respectively. Instead, we use  $\theta$  to denote parameters in general, with the specific meaning inferred from context.

**Conditional Score Estimation in Diffusion Models.** The predicted noise depicted in the previous section is proportional to the score function  $\nabla_{\mathbf{X}_t} \log p_t(\mathbf{X}_t | c)$  (Song et al., 2020; Karras et al., 2024b). Given two distinct conditions,  $c_A$  and  $c_B$ , we can obtain their respective conditional score predictions:

$$\mathbf{S}_A(\mathbf{X}_t, t) = S_{\theta}(\mathbf{X}_t, t, c_A) \quad (4)$$

$$\mathbf{S}_B(\mathbf{X}_t, t) = S_{\theta}(\mathbf{X}_t, t, c_B) \quad (5)$$

Our work aims to generate novel synthetic data augmentations by composing information from two distinct conditional distributions learned by a diffusion model. We achieve this by linearly combining their respective score estimates during the reverse diffusion process.

### 3.1. Synthetic Augmentation via Convex Score Mixing

To generate synthetic samples that interpolate or combine aspects of both  $c_A$  and  $c_B$ , we propose a mixed score  $\mathbf{S}_{\text{mix}}$ :

$$\mathbf{S}_{\text{mix}}(\mathbf{X}_t, t) = \alpha \cdot \mathbf{S}_A(\mathbf{X}_t, t) + \beta \cdot \mathbf{S}_B(\mathbf{X}_t, t) \quad (6)$$

This mixed score  $\mathbf{S}_{\text{mix}}$  is then used to guide the denoising step in a standard reverse diffusion sampler (e.g., DDIM (Song et al., 2020) or a second-order solver as in (Karras et al., 2024b)). Prior works have explored linear combinations of scores for compositional generation, often aiming to satisfy product-of-experts-like objectives or achieve disentangled concept manipulation (Liu et al., 2022; Bradley et al., 2025). These works typically focus on composing disparate concepts (e.g., “object” + “style”) or attributes.

In our work, we adapt this principle specifically for generating *nuanced synthetic augmentations* by mixing related

conditional distributions. We hypothesize that for this application, maintaining the overall magnitude and directional integrity of the score is paramount for generating plausible, on-manifold samples. To the best of our knowledge, this is the first work to systematically investigate and leverage this form of dual-conditional score mixing specifically for the task of generating synthetic data augmentations that lie “between” two defined conditional states, effectively generating hard samples for the discriminator to further boost its discriminative power.

We empirically find that the most plausible and high-fidelity synthetic augmentations are generated when the mixing coefficients  $\alpha$  and  $\beta$  form a convex combination, i.e.,  $\alpha = 1 - \lambda$  and  $\beta = \lambda$  for  $\lambda \in [0, 1]$ . The theoretical rationale for this observation is rooted in several properties of score-based models:

- **Preservation of Expected Score Magnitude.** Diffusion models, particularly those with stabilized training dynamics like EDM2 (Karras et al., 2024b), are trained such that the predicted noise (and thus the score) has an expected magnitude appropriate for the current noise level  $t$ . A convex combination  $\lambda \mathbf{S}_A + (1 - \lambda) \mathbf{S}_B$  inherently averages the directional vectors while being more likely to preserve an overall magnitude consistent with what the model expects. If  $\alpha + \beta \gg 1$ , the resulting score magnitude might become excessively large, akin to an extreme guidance scale in classifier-free guidance (Ho & Salimans, 2021), potentially pushing samples off the manifold. Conversely, if  $\alpha + \beta \ll 1$ , the score magnitude might be too small, leading to under-denoising.
- **Interpolation on the Data Manifold.** The score vectors  $\mathbf{S}_A$  and  $\mathbf{S}_B$  point towards regions of the data manifold consistent with  $c_A$  and  $c_B$ , respectively. A convex combination provides a principled way to interpolate the “denoising force” along paths on this learned manifold. Non-convex combinations could result in update directions that lead to low-density regions or out-of-distribution samples. This will be highlighted empirically in the next section.
- **Factorized Conditionals and Projective Composition.** Recent theoretical work (Bradley et al., 2025) suggests that linear score combinations can provably achieve a desired “projective composition” under certain conditions, such as when the underlying distributions exhibit a factorized conditional structure or can be mapped to such a structure in a feature space. While our conditions  $c_A$  and  $c_B$  may not always strictly satisfy these assumptions (e.g., if they represent entangled attributes), a convex mixing provides the most stable approximation for interpolating between them by maintaining a consistent update scale. Interestingly, as we will highlight in the next section that even though we target identity mixing, the generated samples provably improve the performance of the discriminator.

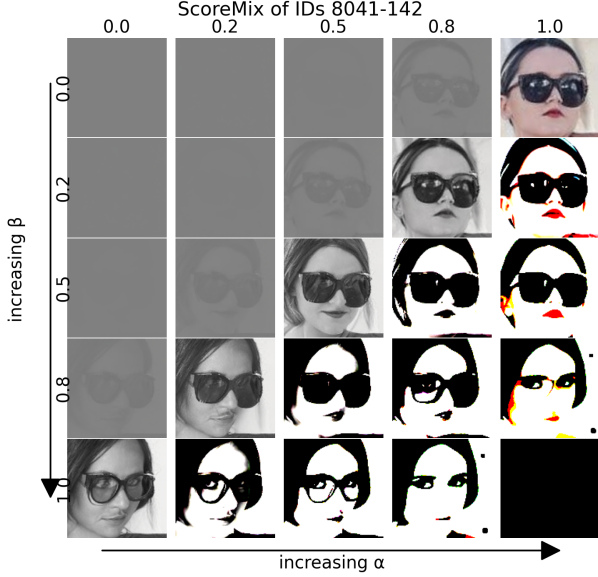


Figure 2. Effect of mixing scores in SCOREMIX. Each cell shows the image produced for one pair of inputs while we sweep the mixing coefficients  $\alpha$  (horizontal axis, increasing left  $\rightarrow$  right) and  $\beta$  (vertical axis, increasing top  $\rightarrow$  bottom). All randomness aspects were fixed for all images

The architectural advancements in models like EDM2 (Karras et al., 2024b), which focus on preserving activation and weight magnitudes, further bolster the argument for convex combinations. If individual conditional scores are already well-calibrated by the model architecture, their convex mix is one of the plausible ways to fuse their guidance without introducing extraneous magnitude distortions.

In Figure 2, the effect of different values of  $\alpha$  and  $\beta$  is depicted. Numeric tick labels give the exact values in steps of 0.2. Here, the class conditional generator is trained using face images in which each class is a unique identity. Arrows beneath and at the side of the grid highlight the directions of increasing influence from each source. The extreme corner corresponds to the unmixed original scores ( $(\alpha, \beta) = (0, 0)$ ) at the top-left and equivalently mixed  $(1, 1)$  at the bottom-right, while the descending diagonal where  $\alpha + \beta = 1$  illustrates the complementary trade-off between the two sources; off-diagonal cells reveal the visual behaviour when the weights do *not* sum to 1, which empirically reflects are previous discussion. Please refer to Subsection A.1 for more qualitative examples.

### 3.2. Sampling Procedure

For generating samples, we employ the deterministic second-order sampler detailed in (Karras et al., 2024b; 2022). At each step  $t$ , the mixed score  $S_{\text{mix}}(\mathbf{X}_t, t)$  from

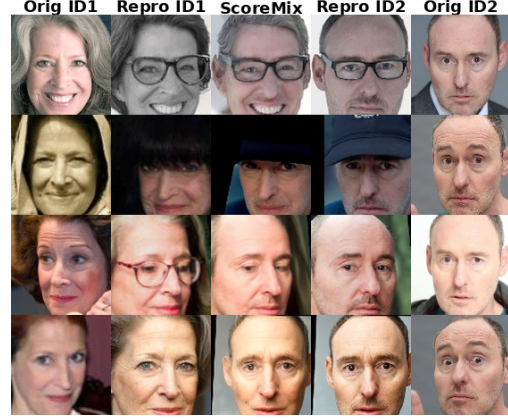


Figure 3. Qualitative comparison of ScoreMix augmentation samples. Each subfigure has five columns: from the left, *Orig ID1* and *Repro ID1* represent samples from the original dataset used to train the generator and their reproductions from the same class using the generator, respectively. Similarly, from the right, *Orig ID2* and *Repro ID2* represent samples from another identity/class. The central column (3rd from the left) shows images generated by mixing scores of ID1 and ID2 according to Equation 6 using AutoGuidance of 1.3. These images serve as augmentations for *Orig ID1* and *Orig ID2* during discriminator training. Note the subtle differences between the **ScoreMix** samples and their source counterparts; we believe these differences contribute significantly to the discriminator’s improved performance beyond architectural enhancements.

Equation 6 is used in place of the single conditional score to compute the update  $\Delta\mathbf{X}_t$ . The specific mixing parameter  $\lambda$  (where  $\alpha = 1 - \lambda, \beta = \lambda$ ) could be varied to generate a spectrum of synthetic augmentations. For simplicity and intuition, we set the  $\lambda = 0.5$ . Given the conditions  $c_A$  and  $c_B$ , the detailed algorithmic procedure for mixing the conditions to generate a plausible mixed image is presented in Algorithm 1. We are also applying autoguidance (Karras et al., 2024a) for sampling, with a model trained with fewer iterations. Some examples of the ScoreMix samples are depicted in the middle column of Figure 3. More examples are in Appendix C.



**Algorithm 1** Sampling with Convex Conditional Score Mixing

---

**Require:** Denoising network  $S_\theta(\mathbf{X}_t, t, \mathbf{c})$ ; conditions  $c_A, c_B$ ; weights,  $\alpha = 0.5, \beta = 0.5$ ; Solver steps  $T$ ,

- 1: Initialize  $\mathbf{X}_t \sim \mathcal{N}(\mathbf{0}, \sigma_T^2 \mathbf{I})$   $\triangleright$  Sample initial noise,  $\sigma_T$  is max noise
- 2: **for**  $t = T$  down to 1 **do**
- 3:    $\mathbf{S}_A \leftarrow S_\theta(\mathbf{X}_t, t, c_A)$   $\triangleright$  Predict noise for A
- 4:    $\mathbf{S}_B \leftarrow S_\theta(\mathbf{X}_t, t, c_B)$   $\triangleright$  Predict noise for B
- 5:    $\mathbf{S}_{\text{mix}} \leftarrow \alpha \cdot \mathbf{S}_A + \beta \cdot \mathbf{S}_B$   $\triangleright$  Convex combination of scores
- 6:    $\mathbf{x}_{t-1} \leftarrow \text{SamplerStep}(\mathbf{X}_t, t, \mathbf{S}_{\text{mix}})$   $\triangleright$  Update using mixed score
- 7: **end for**

**Ensure:** Final generated sample  $\mathbf{x}_0$   $\triangleright$  Output image combining conditions

---

## 4. Experiments

We show that ScoreMix improves face recognition (FR) under limited data, a critical setting given the difficulty of collecting large facial datasets. As FR requires distinguishing between millions of identities, it remains one of the most challenging discriminative tasks, which utilizes SOTA discriminative models that use margin losses (Deng et al., 2019).

### 4.1. Experimental Setup

**Training Data.** For training the generator and the baseline discriminator, we use a subset of WebFace4M (Zhu et al., 2021), referred in (Rahimi et al., 2025) as WebFace160K, was selected to include approximately 10,000 identities (*i.e.*, which is the same order as the other established training datasets like CASIA-WebFace), each represented by 11 to 24 samples, resulting in a total of 160K face images.

**Discriminative Model.** We adopted a standardized baseline. This baseline employed a face recognition (FR) system consisting of an IR50 backbone, modified according to the ArcFace’s implementation (Deng et al., 2019), paired with the ArcFace head (Deng et al., 2019) to incorporate margin loss. Additionally, standard augmentations for face recognition tasks were applied to all models. These augmentations included (1) photometric transformations (2) cropping, and (3) low-resolution adjustments to simulate common variations encountered in real-world scenarios.

**Generative Model.** To train our generative model, we used a variant of the diffusion formulation (Karras et al., 2022; 2024b). For WebFace160K (Rahimi et al., 2025), the subset of WebFace4M (Yi et al., 2014), we used the pixel space variant diffusion models. Furthermore, we set the one-hot condition vectors  $\mathbf{c}^{10K}$ , have a size of  $\sim 10,000$ , corresponding to the number of classes in  $D^{\text{orig}}$ .

### 4.2. Face Recognition Benchmarks

We show that our synthetic augmentation is boosting the performance of a model trained with the real dataset in all of the studied public FR benchmarks. For this purpose, we evaluated against two sets of FR benchmarks. The first set consists of LFW (Huang et al., 2008), CFPFP (Sengupta et al., 2016), CPLFW (Zheng & Deng, 2018), CALFW (Zheng et al., 2017), AgeDB (Moschoglou et al., 2017), which includes mainly high-quality images with various lighting, poses, and ages the average of these benchmarks presented in Table 1 as **Avg-H**. The second set involves benchmarks consisting of medium to low-quality images from a realistic and more challenging FR scenario (NIST IJB-B/C) (Maze et al., 2018; Whitelam et al., 2017) and TinyFace (Cheng et al., 2019). For evaluation, we report verification accuracy (*i.e.*, True Acceptance Rate (TAR)), where the thresholds are set using cross-validation in the high-quality benchmarks, and TARs at different thresholds determined by fixed False Positive Rate (FPR also referred to as False Match Rate in FR literature) in IJB-B/C. Specifically for the latter, we are mainly interested in the verification accuracy for two thresholds that are usually used in real-world scenarios when the FR systems are being deployed, namely  $\text{TAR@FPR}=1\text{-e-}06$  and  $\text{TAR@FPR}=1\text{-e-}05$  for both IJB-B and IJB-C. In the Table 1, the **Aux** column depicts that if the method under study used any auxiliary model for the generation of the dataset other than the  $D^{\text{orig}}$ . The ideal value for this column is **N** which refers to not using any auxiliary model/datasets. The  $n^s$  and  $n^r$  depict the number of synthetic and real images used for training the discriminative model. The double horizontal line groups methods that use CASIA-WebFace or other datasets as the original training data for FR. To control information leakage and validate our first hypothesis, we follow (Rahimi et al., 2025) by using WebFace160K, ensuring a fair comparison; hence, results above and below the line should be considered separately. Furthermore, while ScoreMix requires roughly twice the computation of AugGen for synthetic data generation (10K identities each containing 20 samples), it outperforms AugGen and the discriminator trained on the original dataset for both IR50 and the higher-capacity **IR101** backbones (*i.e.*, note that we are reporting the AugGen and ScoreMix results only using the IR50 backbone, being better than even a discriminator trained using the **IR101** backbone on the original dataset highlights the augmentation can even surpass performance gains we are getting from architectural improvements. From this, we draw the following takeaway:

#### Takeaway

ScoreMixing ( $\lambda = 0.5$ ) can enhance discriminator performance using just a single dataset for synthetic data generation, compared to the original discriminator.

### 4.3. Which classes are best to mix?

In this section, we systematically study which classes are best for approaches like AugGen (Rahimi et al., 2025) or our ScoreMix. By “best,” we mean that the generated samples using the selected classes deliver the highest performance increase compared to the baseline discriminator. To determine this, we first compare the distances between every pair of classes in (i) the learned condition space of the generator and (ii) the embedding space of the discriminator. More precisely, given  $l$  labels in our dataset, we train a discriminator that maps each class to an embedding vector, forming an embedding matrix  $E \in \mathbb{R}^{l \times d_E}$  (i.e., the *learned* class centers used for margin losses). Similarly, for each class we have a unique condition vector that is mapped to the hidden latent of the denoiser network, forming a matrix  $C \in \mathbb{R}^{l \times d_C}$ .

For  $E$ , since it arises from the discriminator’s training, we use *cosine distance* as our metric, which we denote  $\text{dist}_{\text{emb}}$ . For the condition space  $C$ , we experiment with two popular metrics, *cosine distance* and *Euclidean (L2) distance*, both denoted  $\text{dist}_{\text{cond}}$ . This process is depicted in Algorithm 2.

We explore the following hypotheses:

1. Classes that are **closest** in the **embedding** space may be less helpful: because the generator is imperfect, it cannot capture subtle differences between already similar classes, yielding samples that do not challenge the discriminator.
2. Under common metrics (e.g., cosine or L2), interpolating between *closer* conditions may produce better overall samples, potentially improving the discriminator’s performance.
3. A combination: select source classes that are both close in the condition space and distant in the embedding space.

For each setting, we select **10K** class pairs and generate **20** samples per pair, matching the size of the original dataset. Results are shown in Table 2. The “Class Sel Mixing Strategy” column indicates how classes were chosen: *Random* (as in (Rahimi et al., 2025)), or based on their distances.

The first key observation is that adding these augmentations increases average discriminator performance by up to 6%, independent of the mixing strategy. To validate hypothesis (1), we compare strategies based on embedding distances and find that mixing pairs with larger embedding distances yields the greatest gains. In contrast, selecting classes according to condition distances (Close/Dist measured in cosine or  $L_2$ ) has a negligible effect, thereby invalidating hypothesis (2). The critical role of the selection process is also evident from the “Diff.” column of Table 2. For instance, when source classes are chosen by their embedding-space distances, the mean pairwise distance is 2.52—substantially higher than the 0.11 or 0.56 observed in condition

space—highlighting the importance of sampling in embedding space. (3) Finally advantages of selection based on the two spaces together, as presented in the *Top/Worst Close Cond, Dist Embed*, do not reach the gains achieved through selection based on the embedding space solely.

#### Takeaway

Choosing the source classes according to their distance based on the **Embedding** space *under common distances* has more impact on the performance increase of the discriminator. The **most distant** classes are the most effective ones.

#### Algorithm 2 DISTANCECORRELATION

**Require:** embedding matrix  $E \in \mathbb{R}^{l \times d_E}$ , Embedding Space distance function  $\text{dist}_{\text{emb}}(\cdot, \cdot)$  condition matrix  $C \in \mathbb{R}^{l \times d_C}$ , Condition Space distance function  $\text{dist}_{\text{cond}}(\cdot, \cdot)$

**Ensure:**  $c$  and  $e$

- 1:  $e \leftarrow []$  ▷ distances in  $E$ -space
- 2:  $c \leftarrow []$  ▷ distances in  $C$ -space
- 3: **for**  $i \leftarrow 1$  **to**  $l - 1$  **do**
- 4:   **for**  $j \leftarrow i + 1$  **to**  $l$  **do**
- 5:      $e \leftarrow \text{dist}_{\text{emb}}(E_{:,i}, E_{:,j})$
- 6:      $c \leftarrow \text{dist}_{\text{cond}}(C_{:,i}, C_{:,j})$
- 7:     append  $u$  to  $\mathbf{u}$ ; append  $v$  to  $\mathbf{v}$
- 8:   **end for**
- 9: **end for**
- 10:

**Learned Discriminator Features as Generators Condition.** As highlighted previously, under usual metrics, there is no clear correspondence between the discriminators’ embedding space and the learned generator’s condition space, please refer to Appendix B for more information. This gives us the idea to initialize the generator’s condition space using the discriminators’ class centers and freezing them to observe if we can enforce the missing correspondence. We quickly figure that this approach is not feasible, leading to the generators’ failure to converge.

#### Takeaway

Diffusion generators tend not to converge or produce plausible results when we use the discriminators’ features as the frozen conditions. This is done to enforce the known structure of the embedding space.

## 5. Conclusions

In this work, we demonstrate that we can leverage the Score Compositional properties of diffusion models to enhance the performance of the discriminator. The performance increase exceeds what can be achieved by more parameterized discrimination, highlighting the promises of synthetic augmentation for boosting the performance. We also studied

Table 1. Comparison of the  $FR_{syn}$  training (upper part),  $FR_{real}$  training (middle), and  $FR_{mix}$  training (bottom) using CASIA-WebFace/WebFace160K, when the models are evaluated in terms of accuracy against standard FR benchmarks. **Avg-H** depicts the average accuracy of all high-quality benchmarks including, LFW, CFP-FP, CPLFW, AgeDB, and CALFW. Here  $n^s$  and  $n^r$  depict the number of Synthetic and Real Images respectively and Aux depicts whether the method for generating the dataset uses an auxiliary information network for generating their datasets (**Y**) or not (**N**). The  $\dagger$  denotes network trained on **IR101** if not the model trained using the IR50. The numbers under columns labeled like C/B-1e-6 indicate TAR for IJB-C/B at FPR of 1e-6. TR1 depicts the rank-1 accuracy for the TinyFace benchmark.

Method/Data	Aux	$n^s$	$n^r$	B-1e-6	B-1e-5	C-1e-6	C-1e-5	TR1	Avg-H
DigiFace1M	N/A	1.2M	0	15.31	29.59	26.06	36.34	32.30	78.97
RealDigiFace	<b>Y</b>	1.2M	0	21.37	39.14	36.18	45.55	42.64	81.34
DCFace	<b>Y</b>	1.2M	0	22.48	47.84	35.27	58.22	45.94	91.56
AugGen	<b>N</b>	0.6M	0	<b>29.40</b>	<b>54.54</b>	<b>45.15</b>	<b>61.52</b>	52.33	88.78
AugGen Repro	<b>N</b>	0.6M	0	15.71	45.97	31.54	58.61	53.61	90.64
CASIA-WebFace	N/A	0	0.5M	1.02	5.06	0.73	5.37	58.12	94.21
CASIA-WebFace $\dagger$	N/A	0	0.5M	0.74	3.94	0.38	3.92	<b>59.64</b>	<b>94.84</b>
WebFace160K	N/A	0	0.16M	32.13	72.18	70.37	78.81	61.51	92.50
WebFace160K $\dagger$	N/A	0	0.16M	34.84	74.10	72.56	81.26	62.59	93.32
ScoreMix (Ours)	<b>N</b>	0.2M	0	28.15	57.71	54.66	67.06	56.38	92.47
AugGen	<b>N</b>	0.2M	0.16M	34.83	76.21	75.02	82.91	61.41	93.78
ScoreMix (Ours)	<b>N</b>	0.2M	0.16M	<b>35.95</b>	<b>76.41</b>	<b>76.45</b>	<b>83.58</b>	<b>63.09</b>	<b>93.87</b>

Table 2. Effect of different strategies for choosing classes to mix for generating augmentations for enhancing the discriminator’s performance. Here *Class Sel Mixing Strategy* refers to how we select the classes to mix for the final generation. All networks were trained using a normalized IR50 backbone with an ArcFace head. The numbers under columns labeled like C/B-1e-6 indicate TAR for IJB-C/B at FPR of 1e-6. TR1,5 depicts the rank-1,5 accuracy for the TinyFace benchmark. The Avg column is the average of all reported metrics, for each two rows grouped together (e.g., **Close Embedding Cosine** and **Dist Embedding Cosine** the *Diff* column depicts the absolute difference of the average metrics, presenting the effectiveness of the studied selection strategy.

Class Sel Mixing Strategy	$n^s$	$n^r$	B-1e-6	B-1e-5	C-1e-6	C-1e-5	TR1	TR5	Avg	Diff.
WebFace160K	0	0.16M	33.15	72.54	70.42	78.62	61.51	66.68	63.82	N/A
Random	0.2M	0.16M	34.83	76.21	75.02	82.91	61.41	66.60	66.17	N/A
Close Embedding Cosine	0.2M	0.16M	34.78	73.12	71.86	81.00	61.91	66.82	64.92	<b>2.52</b>
Dist Embedding Cosine	0.2M	0.16M	34.42	<b>77.46</b>	<b>78.62</b>	<b>84.04</b>	<b>62.66</b>	67.46	<b>67.44</b>	
Close Condition Cosine	0.2M	0.16M	<b>37.61</b>	76.38	74.43	82.71	62.29	<b>67.65</b>	66.84	0.11
Dist Condition Cosine	0.2M	0.16M	34.52	77.17	76.97	83.15	62.39	67.49	66.95	
Close Condition L2	0.2M	0.16M	37.18	72.67	72.20	80.71	62.12	66.52	65.23	0.56
Dist Condition L2	0.2M	0.16M	33.34	75.63	75.82	82.02	61.61	66.34	65.79	
Top Close Cond, Dist Embed	0.2M	0.16M	34.74	76.94	76.70	83.87	62.47	67.14	66.98	1.76
Worst Close Cond, Dist Embed	0.2M	0.16M	33.27	74.45	74.50	81.22	61.13	66.77	65.22	

which classes are more usable for this task, and lastly, we observed that under a common distance metrics, there is no clear correlation between the learned generator’s condition space and the discriminator’s feature space.

**Limitations.** Although our method does not require grid search and usage of the discriminator (i.e., even the one trained on the same dataset), unlike AugGen (Rahimi et al., 2025), its downside is that while sampling, the computational cost is effectively two times that of AugGen (in case

we mainly mix two identities), making it slower for larger-scale synthetic generation in comparison to AugGen.

**Future work.** An interesting direction for future research is to explore the effect of mixing more than two identities. It remains to be seen whether incorporating different mixtures can further enhance the discriminator’s performance. Additionally, instead of freezing the condition space, it would be interesting to see what will happen if we properly regularize the space to have the same topology as the desired space

(i.e., embedding space of the discriminator in our case).

**Acknowledgment.** This research is based on work conducted in the SAFER project and supported by the Hasler Foundation’s Responsible AI program.

## References

- Anderson, B. D. Reverse-time diffusion equation models. *Stochastic Processes and their Applications*, 12(3):313–326, 1982.
- Azizi, S., Kornblith, S., Saharia, C., Norouzi, M., and Fleet, D. J. Synthetic data from diffusion models improves imagenet classification. *Transactions on Machine Learning Research*, 2023. ISSN 2835-8856. URL <https://openreview.net/forum?id=DlRsoxjyPm>.
- Bae, G., de La Gorce, M., Baltrušaitis, T., Hewitt, C., Chen, D., Valentin, J., Cipolla, R., and Shen, J. Digiface-1m: 1 million digital face images for face recognition. In *Proceedings of the IEEE/CVF Winter Conference on Applications of Computer Vision*, pp. 3526–3535, 2023.
- Blanz, V. and Vetter, T. A morphable model for the synthesis of 3d faces. In *Proceedings of the 26th Annual Conference on Computer Graphics and Interactive Techniques, SIGGRAPH ’99*, pp. 187–194, USA, 1999. ACM Press/Addison-Wesley Publishing Co. ISBN 0201485605. doi: 10.1145/311535.311556. URL <https://doi.org/10.1145/311535.311556>.
- Bradley, A., Nakkiran, P., Berthelot, D., Thornton, J., and Susskind, J. M. Mechanisms of projective composition of diffusion models. *arXiv preprint arXiv:2502.04549*, 2025.
- Cheng, Z., Zhu, X., and Gong, S. Low-resolution face recognition. In *Computer Vision—ACCV 2018: 14th Asian Conference on Computer Vision, Perth, Australia, December 2–6, 2018, Revised Selected Papers, Part III 14*, pp. 605–621. Springer, 2019.
- Deng, J., Guo, J., Xue, N., and Zafeiriou, S. Arcface: Additive angular margin loss for deep face recognition. In *Proceedings of the IEEE/CVF conference on computer vision and pattern recognition*, pp. 4690–4699, 2019.
- Esser, P., Rombach, R., and Ommer, B. Taming transformers for high-resolution image synthesis. In *Proceedings of the IEEE/CVF conference on computer vision and pattern recognition*, pp. 12873–12883, 2021.
- Esser, P., Kulal, S., Blattmann, A., Entezari, R., Müller, J., Saini, H., Levi, Y., Lorenz, D., Sauer, A., Boesel, F., et al. Scaling rectified flow transformers for high-resolution image synthesis. In *Forty-first International Conference on Machine Learning*, 2024.
- Frid-Adar, M., Klang, E., Amitai, M., Goldberger, J., and Greenspan, H. Synthetic data augmentation using gan for improved liver lesion classification. In *2018 IEEE 15th International Symposium on Biomedical Imaging (ISBI 2018)*, pp. 289–293, 2018. doi: 10.1109/ISBI.2018.8363576.

- Ho, J. and Salimans, T. Classifier-free diffusion guidance. In *NeurIPS 2021 Workshop on Deep Generative Models and Downstream Applications*, 2021. URL <https://openreview.net/forum?id=qw8AKxfYbI>.
- Huang, G. B., Mattar, M., Berg, T., and Learned-Miller, E. Labeled faces in the wild: A database for studying face recognition in unconstrained environments. In *Workshop on faces in 'Real-Life' Images: detection, alignment, and recognition*, 2008.
- Karras, T., Aittala, M., Aila, T., and Laine, S. Elucidating the design space of diffusion-based generative models. *Advances in neural information processing systems*, 35: 26565–26577, 2022.
- Karras, T., Aittala, M., Kynkäänniemi, T., Lehtinen, J., Aila, T., and Laine, S. Guiding a diffusion model with a bad version of itself. *Advances in Neural Information Processing Systems*, 37:52996–53021, 2024a.
- Karras, T., Aittala, M., Lehtinen, J., Hellsten, J., Aila, T., and Laine, S. Analyzing and improving the training dynamics of diffusion models. In *Proc. CVPR*, 2024b.
- Kim, M., Liu, F., Jain, A., and Liu, X. Dcfac: Synthetic face generation with dual condition diffusion model. In *Proceedings of the IEEE/CVF Conference on Computer Vision and Pattern Recognition*, pp. 12715–12725, 2023.
- Kupyn, O. and Rupperecht, C. Dataset enhancement with instance-level augmentations. *arXiv preprint arXiv:2406.08249*, 2024.
- Labs, B. F. Flux. <https://github.com/black-forest-labs/flux>, 2024.
- Lee, S., Kreis, K., Veccham, S. P., Liu, M., Reidenbach, D., Peng, Y., Paliwal, S., Nie, W., and Vahdat, A. Genmol: A drug discovery generalist with discrete diffusion. *arXiv preprint arXiv:2501.06158*, 2025.
- Liu, N., Li, S., Du, Y., Torralba, A., and Tenenbaum, J. B. Compositional visual generation with composable diffusion models. In *European Conference on Computer Vision*, pp. 423–439. Springer, 2022.
- Maze, B., Adams, J., Duncan, J. A., Kalka, N., Miller, T., Otto, C., Jain, A. K., Niggel, W. T., Anderson, J., Cheney, J., et al. Iarpa janus benchmark-c: Face dataset and protocol. In *2018 international conference on biometrics (ICB)*, pp. 158–165. IEEE, 2018.
- Moschoglou, S., Papaioannou, A., Sagonas, C., Deng, J., Kotsia, I., and Zafeiriou, S. Agedb: the first manually collected, in-the-wild age database. In *proceedings of the IEEE conference on computer vision and pattern recognition workshops*, pp. 51–59, 2017.
- Peebles, W. and Xie, S. Scalable diffusion models with transformers. In *Proceedings of the IEEE/CVF international conference on computer vision*, pp. 4195–4205, 2023.
- Qiu, H., Yu, B., Gong, D., Li, Z., Liu, W., and Tao, D. Synface: Face recognition with synthetic data. In *Proceedings of the IEEE/CVF International Conference on Computer Vision*, pp. 10880–10890, 2021.
- Rahimi, P., Ecabert, C., and Marcel, S. Toward responsible face datasets: modeling the distribution of a disentangled latent space for sampling face images from demographic groups. In *2023 IEEE International Joint Conference on Biometrics (IJCB)*, pp. 1–11. IEEE, 2023.
- Rahimi, P., Razeghi, B., and Marcel, S. Synthetic to authentic: Transferring realism to 3d face renderings for boosting face recognition. *arXiv preprint arXiv:2407.07627*, 2024.
- Rahimi, P., Teney, D., and Marcel, S. Auggen: Synthetic augmentation can improve discriminative models. *arXiv preprint arXiv:2503.11544*, 2025.
- Russakovsky, O., Deng, J., Su, H., Krause, J., Satheesh, S., Ma, S., Huang, Z., Karpathy, A., Khosla, A., Bernstein, M., Berg, A. C., and Fei-Fei, L. ImageNet Large Scale Visual Recognition Challenge. *International Journal of Computer Vision (IJCV)*, 115(3):211–252, 2015. doi: 10.1007/s11263-015-0816-y.
- Sengupta, S., Chen, J.-C., Castillo, C., Patel, V. M., Chellappa, R., and Jacobs, D. W. Frontal to profile face verification in the wild. In *2016 IEEE winter conference on applications of computer vision (WACV)*, pp. 1–9. IEEE, 2016.
- Sevastopolskiy, A., Malkov, Y., Durasov, N., Verdoliva, L., and Nießner, M. How to boost face recognition with stylegan? In *Proceedings of the IEEE/CVF International Conference on Computer Vision*, pp. 20924–20934, 2023.
- Song, J., Meng, C., and Ermon, S. Denoising diffusion implicit models. *arXiv preprint arXiv:2010.02502*, 2020.
- Whitelam, C., Taborsky, E., Blanton, A., Maze, B., Adams, J., Miller, T., Kalka, N., Jain, A. K., Duncan, J. A., Allen, K., et al. Iarpa janus benchmark-b face dataset. In *proceedings of the IEEE conference on computer vision and pattern recognition workshops*, pp. 90–98, 2017.
- Wood, E., Baltrušaitis, T., Hewitt, C., Dziadzio, S., Cashman, T. J., and Shotton, J. Fake it till you make it: face analysis in the wild using synthetic data alone. In *Proceedings of the IEEE/CVF international conference on computer vision*, pp. 3681–3691, 2021.



- Xu, J., Li, S., Wu, J., Xiong, M., Deng, A., Ji, J., Huang, Y., Mu, G., Feng, W., Ding, S., et al. Id<sup>3</sup>: Identity-preserving-yet-diversified diffusion models for synthetic face recognition. In *The Thirty-eighth Annual Conference on Neural Information Processing Systems*, 2024.
- Yeung, M., Teramoto, T., Wu, S., Fujiwara, T., Suzuki, K., and Kojima, T. Variface: Fair and diverse synthetic dataset generation for face recognition. *arXiv preprint arXiv:2412.06235*, 2024.
- Yi, D., Lei, Z., Liao, S., and Li, S. Z. Learning face representation from scratch. *arXiv preprint arXiv:1411.7923*, 2014.
- Zheng, T. and Deng, W. Cross-pose lfw: A database for studying cross-pose face recognition in unconstrained environments. *Beijing University of Posts and Telecommunications, Tech. Rep*, 5(7), 2018.
- Zheng, T., Deng, W., and Hu, J. Cross-age lfw: A database for studying cross-age face recognition in unconstrained environments. *arXiv preprint arXiv:1708.08197*, 2017.
- Zhu, Z., Huang, G., Deng, J., Ye, Y., Huang, J., Chen, X., Zhu, J., Yang, T., Lu, J., Du, D., et al. Webface260m: A benchmark unveiling the power of million-scale deep face recognition. In *Proceedings of the IEEE/CVF Conference on Computer Vision and Pattern Recognition*, pp. 10492–10502, 2021.

## A. Appendix

### A.1. ScoreMixing

In the figures Figure 4, Figure 5 and Figure 6 more examples of different values of  $\alpha$  and  $\beta$  are depicted. For each panel, the ID combinations are fixed across the figures to also highlight the consistency of the IDs with different sources of randomness. Note that the initial value of the seeds was all fixed for each figure to mainly study the effects of mixes of the conditions and the effects of the different values of the  $\alpha$  and  $\beta$ .

## B. Illustration of Embedding and Condition Space

After normalizing and identifying the most similar pairs (i.e., those with cosine distance 0, or equivalently, cosine similarity 1), we shift these zero distances to  $-1$  to improve visual contrast. The resulting distance matrices for all sample pairs,  $\mathbf{E}$  and  $\mathbf{C}$ , are shown in Figure 7. From these plots, we see no obvious correlation between the two spaces.

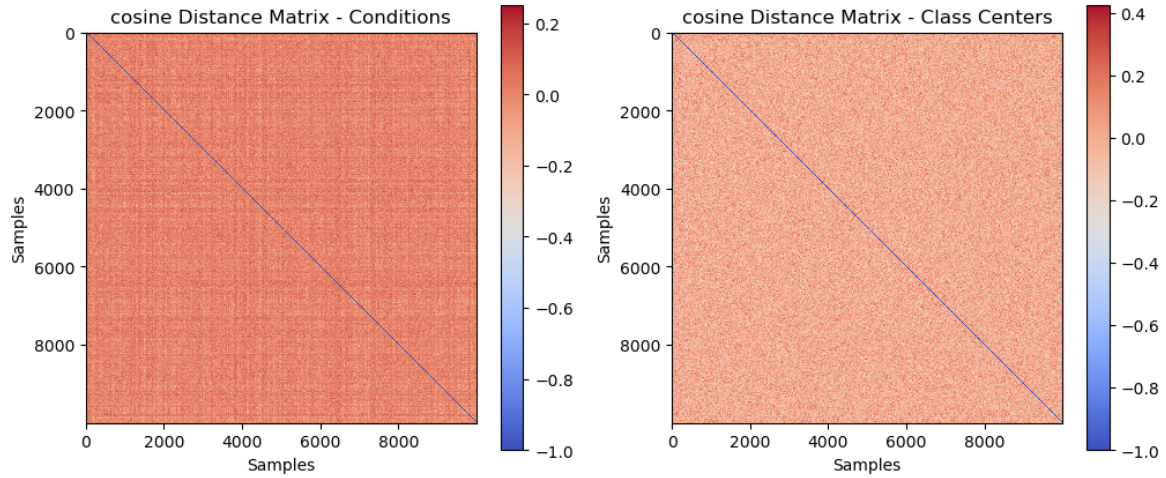


Figure 7. Shifted Matrix Cosine Matrix Distances between each pair in the condition and embedding space.

As another way of viewing this, if we flatten the matrices and use a few pairs like a set  $\mathcal{S}$ :

$$\mathcal{S} \subseteq \{1, \dots, 10000\} \times \{1, \dots, 10000\}, \quad (i, j) \in \mathcal{S}.$$

And treating the distances as a 1D signal where each tick of the x-axis corresponds to a unique combination of  $i$  and  $j$ , we get a plot like Figure 8. Here, the red vertical lines are illustrating when the both condition and embedding space are having a distance lower than 0.4. We also apply some peak detection especially for the embedding space as we demonstrated the more distant we have in the embedding space the more beneficial the synthetic samples will be. Here, we again observe that these two spaces do not correlate well.

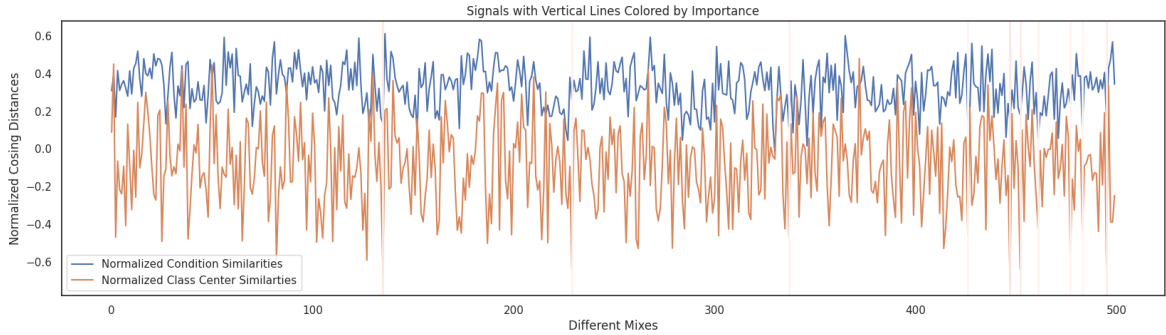


Figure 8. Selected few distances in condition and embedding space. Here x-axis depicts a few unique combinations of classes.

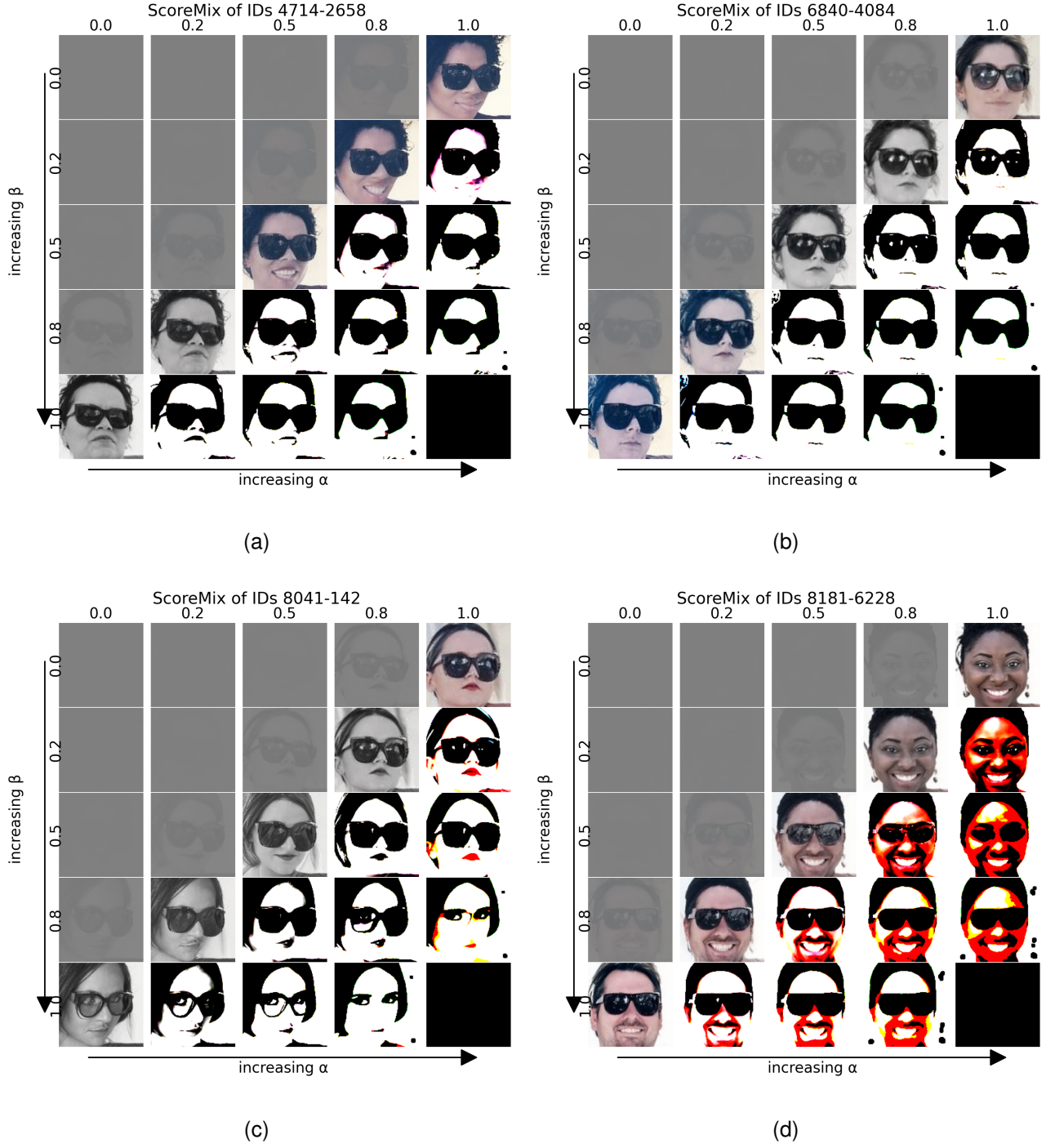


Figure 4. Effect of mixing scores in SCOREMIX. Subfigures a–d show the images obtained for four different input pairs while sweeping the mixing coefficients  $\alpha$  (horizontal axis, *increasing left  $\rightarrow$  right*) and  $\beta$  (vertical axis, *increasing top  $\rightarrow$  bottom*). All randomness aspects were fixed. All images were generated by fixing all the seeds to the initial value of ‘0’.

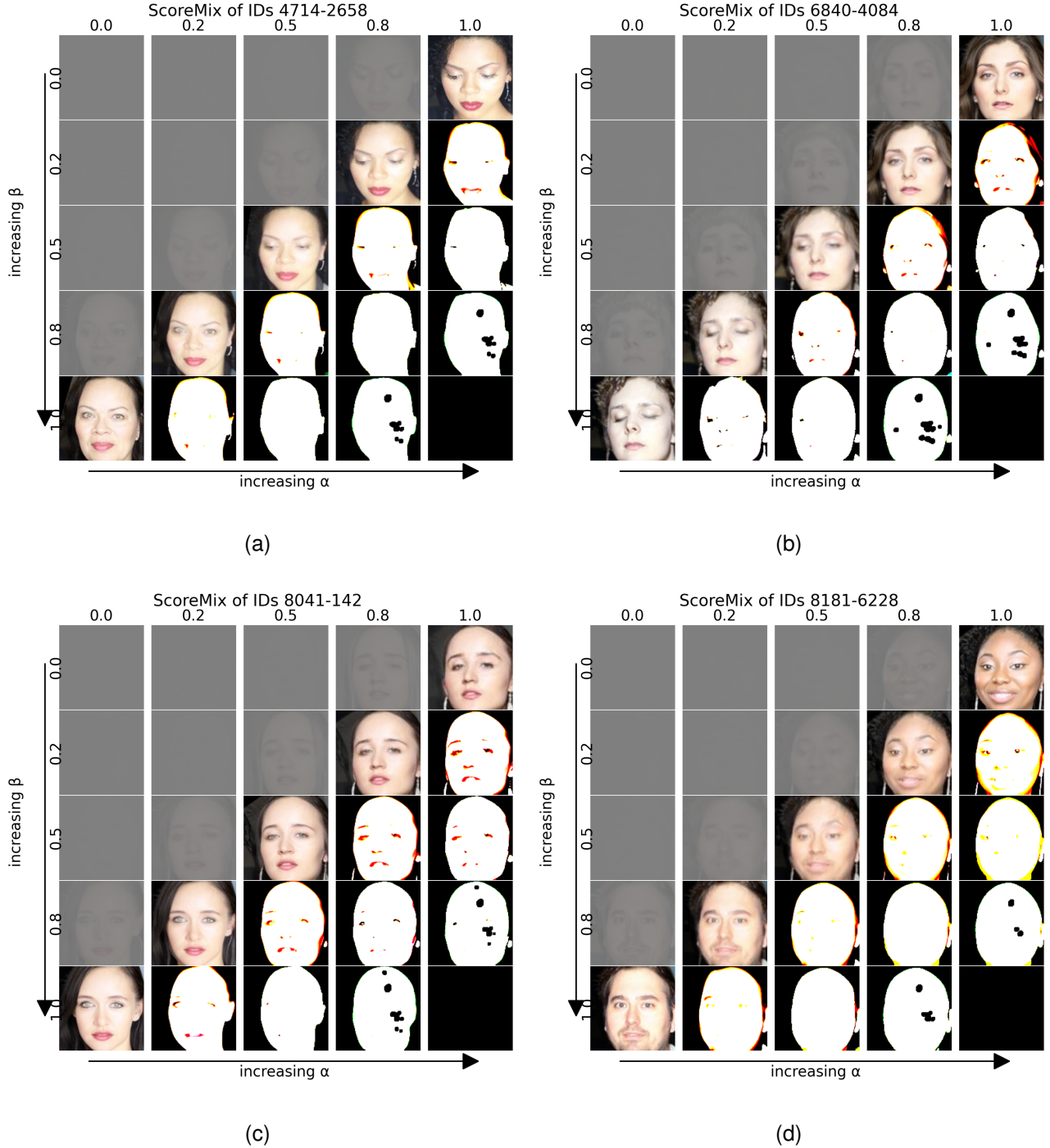


Figure 5. Effect of mixing scores in SCOREMIX. Subfigures a–d show the images obtained for four different input pairs while sweeping the mixing coefficients  $\alpha$  (horizontal axis, *increasing left  $\rightarrow$  right*) and  $\beta$  (vertical axis, *increasing top  $\rightarrow$  bottom*). All randomness aspects were fixed. All images were generated by fixing all the seeds to the initial value of ‘1’.

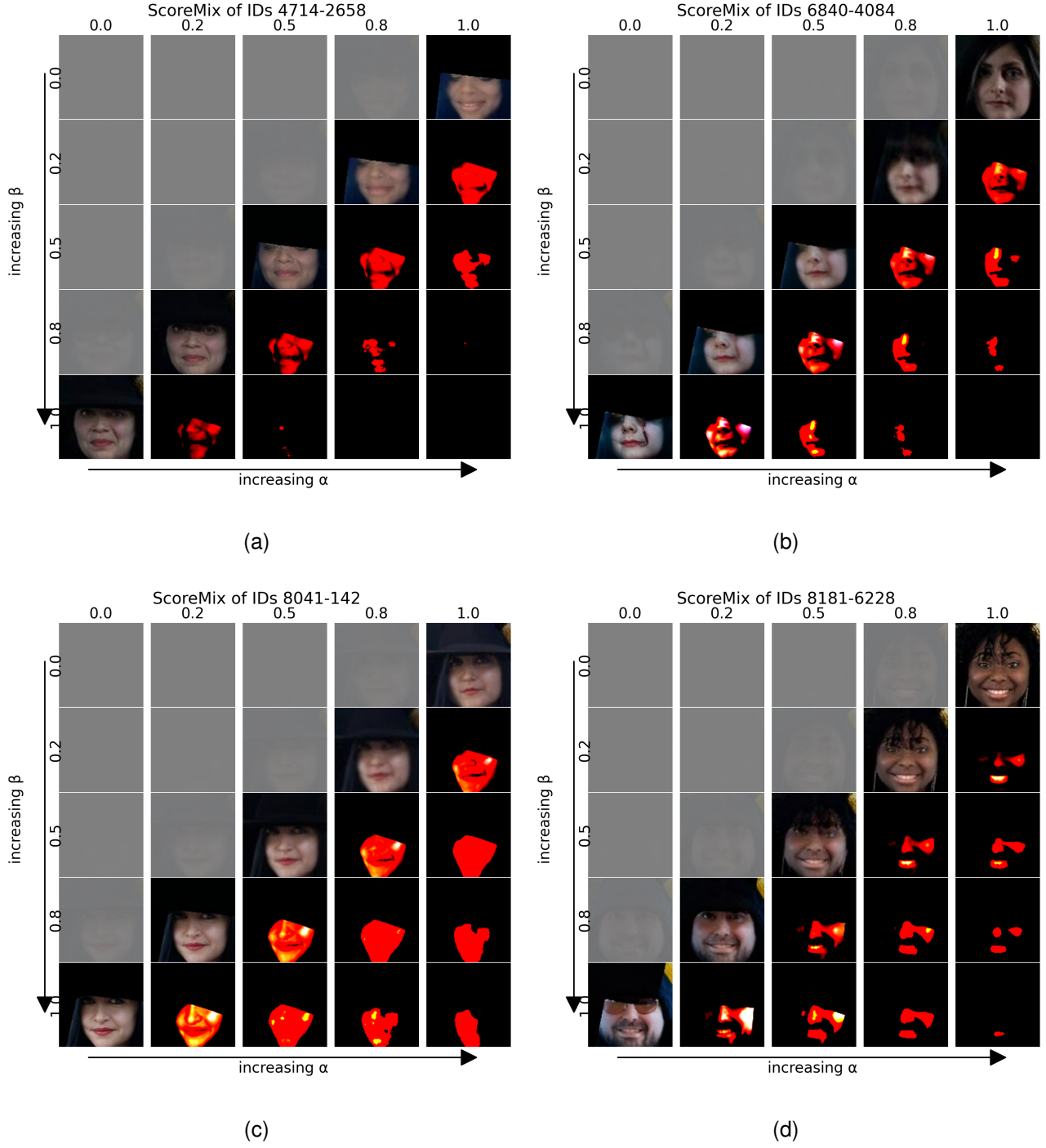
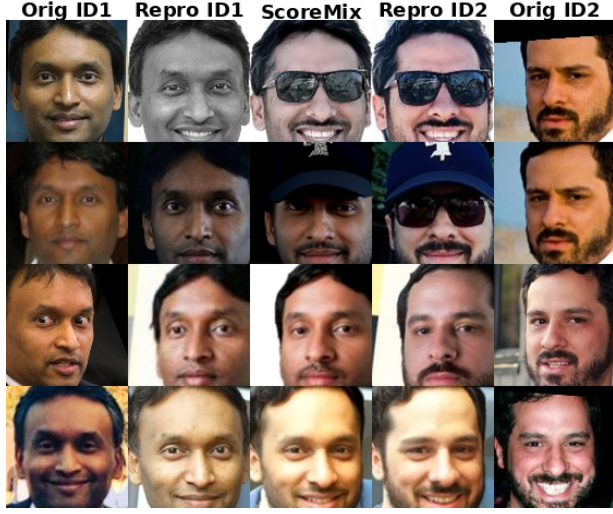


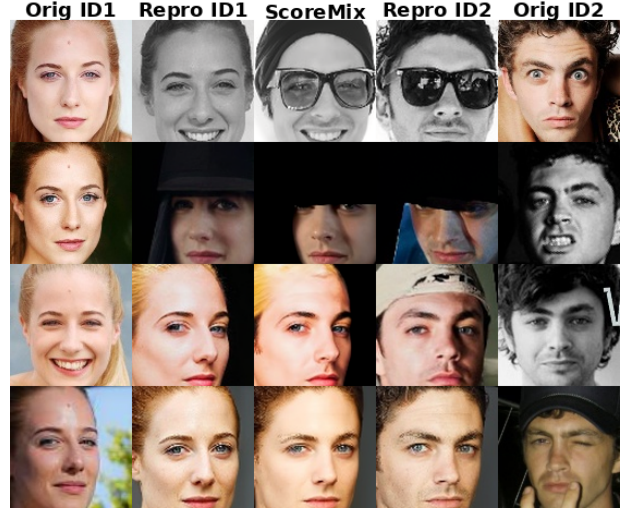
Figure 6. Effect of mixing scores in SCOREMIX. Subfigures a–d show the images obtained for four different input pairs while sweeping the mixing coefficients  $\alpha$  (horizontal axis, *increasing left  $\rightarrow$  right*) and  $\beta$  (vertical axis, *increasing top  $\rightarrow$  bottom*). All randomness aspects were fixed. All images were generated by fixing all the seeds to the initial value of ‘6’.



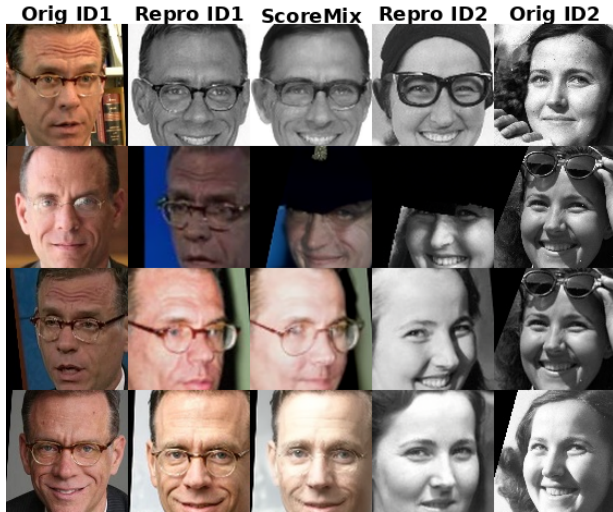
## C. ScoreMix Samples



(a) IDs 6934 and 2767



(b) IDs 4566 and 2325



(c) IDs 8430 and 5412



(d) IDs 8476 and 2790

Figure 9. Qualitative comparison of ScoreMix augmentation samples. Each subfigure has five columns: from the left, *Orig ID1* and *Repro ID1* represent samples from the original dataset used to train the generator and their reproductions from the same class using the generator, respectively. Similarly, from the right, *Orig ID2* and *Repro ID2* represent samples from another identity/class. The central column (3rd from the left) shows images generated by mixing scores of ID1 and ID2 according to Equation 6 using AutoGuidance of 1.3. These images serve as augmentations for *Orig ID1* and *Orig ID2* during discriminator training. Note the subtle differences between the **ScoreMix** samples and their source counterparts; we believe these differences contribute significantly to the discriminator’s improved performance beyond architectural enhancements.

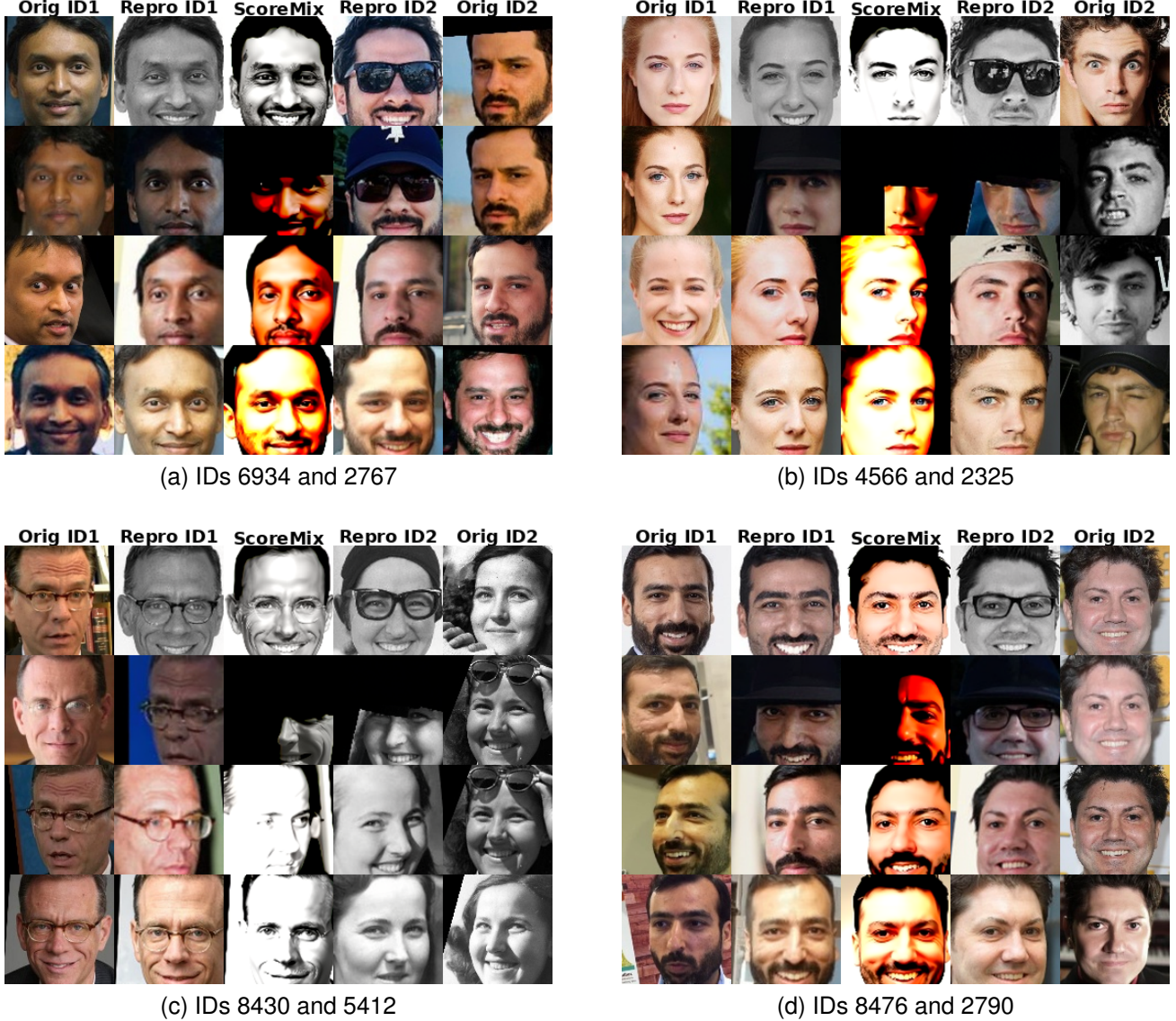


Figure 10. Qualitative comparison of ScoreMix augmentation samples. Each subfigure has five columns: from the left, *Orig ID1* and *Repro ID1* represent samples from the original dataset used to train the generator and their reproductions from the same class using the generator, respectively. Similarly, from the right, *Orig ID2* and *Repro ID2* represent samples from another identity/class. The central column (3rd from the left) shows images generated by mixing scores of ID1 and ID2 according to Equation 6 using AutoGuidance of 2.75. These images serve as augmentations for *Orig ID1* and *Orig ID2* during discriminator training. Note the subtle differences between the **ScoreMix** samples and their source counterparts; we believe these differences contribute significantly to the discriminator’s improved performance beyond architectural enhancements.